Structure of O/Fe(001)-p(1×1) studied by surface x-ray diffraction

S. S. Parihar,[1] H. L. Meyerheim,[1,*] K. Mohseni,[1] S. Ostanin,[1] A. Ernst,[1] N. Jedrecy,[2] R. Felici,[3] and J. Kirschner[1]
[1]*Max-Planck-Institut für Mikrostrukturphysik, Weinberg 2, D-06120 Halle, Germany*
[2]*Institut des Nano Sciences de Paris, Université Pierre et Marie Curie-Paris 6 and CNRS, UMR 7588, 75015 Paris, France*
[3]*ESRF, BP 220, F-38043 Grenoble Cedex, France*
(Received 3 December 2009; published 23 February 2010)

The geometric structure of O/Fe(001)-p(1×1) is studied by surface x-ray diffraction (SXRD). After dosing of about 4 L (1 L=10^{-6} Torr s) of oxygen at room temperature we find approximately one monolayer (ML) of oxygen in an FeO-like structure forming two layer thick islands covering about 40% of a roughened Fe(001) surface. Subsequent annealing up to 500 °C results in surface flattening leading to a highly ordered structure. Very precise SXRD data reveal the presence of 1 ML of oxygen atoms located in fourfold hollow sites at $d_{(\text{O-Fe})}=0.48\pm0.08$ Å above the first Fe layer. The first Fe–Fe-interlayer spacing is expanded to $d_{12}=1.66\pm0.02$ Å corresponding to an increase of 16% relative to the bulk spacing (1.43 Å). Density-functional calculations confirm our findings and indicate a strong dependence of the (local) layer expansion on the oxygen coverage. Our results are important for understanding the surface magnetic properties of the O/Fe(001)-p(1×1) surface in general.

DOI: 10.1103/PhysRevB.81.075428 PACS number(s): 68.35.Ct, 61.05.cp, 68.47.Gh, 71.15.Mb

I. INTRODUCTION

Adsorption of a foreign species on a crystal surface usually induces atomic relaxations and modifications of the surface electronic states thereby affecting the surface physical and chemical properties. In this context, the O/Fe(001)-p(1×1) structure is an intensely studied model system because of the oxygen adsorption induced enhancement of the surface magnetic moments and the increased exchange splitting.[1–7] More recently this property has motivated the development of a new detector for spin analysis.[8]

Already in 1985, the enhancement of the surface magnetic moment was attributed to the oxygen induced expansion of the top Fe-interlayer spacing (d_{12}).[1] Later, optical surface second-harmonic generation[6] and spin-polarized metastable de-excitation spectroscopy[4] experiments showed the direct correlation between the surface magnetic signal and the Fe coverage during subsequent Fe deposition on the O/Fe(001)-p(1×1) surface, thereby taking advantage of the surfactant effect. In these experiments, maxima were observed for complete Fe layers, where the O/Fe(001)-p(1×1) hollow site geometry is restored with a maximum value of d_{12}. A very recent study combining spin-polarized scanning tunneling microscopy (STM) with first-principles calculations[7] identified the oxygen adsorption induced stabilization of the ferromagnetism of the Fe(001) surface involving a positive spin polarization at the Fermi level.

Despite its decisive influence on the surface magnetic properties surprisingly little is known about the geometric structure of the O/Fe(001)-p(1×1) surface. Moreover, studies published so far are considerably contradictory. More than 30 years ago the first low-energy electron diffraction (LEED) (Ref. 9) study concluded that oxygen atoms reside in fourfold hollow sites at a vertical distance $d_{(\text{O-Fe})}=0.48$ Å above the top Fe layer. An outward 7.5% expansion of d_{12} to 1.54 Å was found as compared to the bulk spacing of 1.43 Å. While a later study by the same group[10] confirmed this result, it is at variance with the theoretical work of Chubb and Pickett,[11] who found a considerably stronger expansion of +23% (1.76 Å), but a smaller value of $d_{(\text{O-Fe})}$ (0.38 Å).

In a more recent first-principles theoretical study the spacing d_{12} was determined to be 1.66 Å and the distance between the oxygen layer and the iron surface was derived to be 0.45 Å (Ref. 3). A medium energy ion scattering study by Headrick *et al.*[12] determined $d_{12}=1.59$ Å (+11%), but no oxygen adsorption height was reported.

A similar ambiguity also exists with regard to the oxygen exposure necessary to saturate the Fe(001) surface and to form a well-ordered p(1×1) structure. Saturation is commonly attributed to the adsorption of one monolayer (ML) of oxygen atoms corresponding to 1.2×10^{15} atoms/cm^2. It corresponds to a minimum in the oxygen sticking coefficient, which experimentally is identified with a plateau (kink) in the intensity ratios between electron spectroscopy emission lines of oxygen and Fe,[9,12–16] work function maximum,[13] and/or the maximization of characteristic LEED reflection intensities.[9] Reports vary between 0.6 L (1 L=10^{-6} Torr s) [15] and 6 L.[9] Based on electron energy-loss spectroscopy, Sakisaka *et al.*[17] suggested three different stages of the O/Fe(001) interface formation: (i) dissociative chemisorption up to 3 L followed by (ii) incorporation of oxygen adatoms into the selvedge between 3 and 20 L and (iii) oxide formation above 20 L.

One may speculate that the disparity of the oxygen exposure values needed to prepare a saturated oxygen p(1×1) surface structure is due to the absence of a sharp transition between the different stages of interface formation. Also, the density of structural defects and the experimental conditions (e.g., sample temperature) might have a strong influence on the adsorption kinetics. But according to Lu *et al.*,[14] sample heating at 650 °C annihilates any surface disorder induced by overdosing and leads to an ordered and oxygen saturated O/Fe(001)-p(1×1) structure. Later studies on the surface magnetic properties followed this procedure by dosing up to 30 L followed by annealing at 620–670 °C.[4–7]

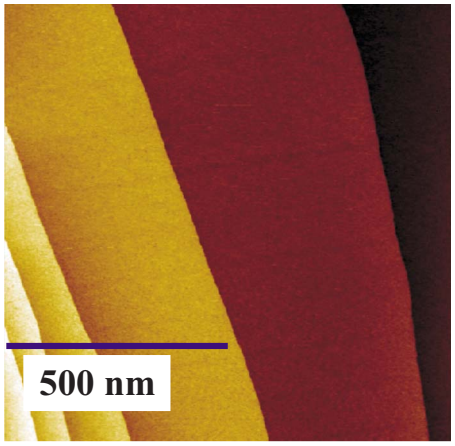

FIG. 1. (Color online) 1000×1000 nm^2 STM image of Fe(001) surface.

The present situation calls for a precise determination of the O/Fe(001)-p(1×1) atomic geometry. Surface x-ray diffraction (SXRD) has become an important tool for the analysis of surfaces and interfaces, mostly because the data analysis is based on single scattering theory. Moreover, third generation synchrotron facilities delivering highly brilliant x rays allow the collection of reflection intensities sufficiently large in number and accurate enough to determine fractions of a ML of low-Z atoms such as oxygen. It should be emphasized that one prerequisite is the preparation of a high-quality sample in terms of long-range order.

In this study we present a precise SXRD analysis of the O/Fe(001)-p(1×1) adsorption geometry. The paper is outlined as follows. In Sec. II we shortly outline the experimental procedures, while Sec. III discusses in detail the structures determined for the sample after oxygen deposition ("as deposited" and after annealing). Section IV presents the first-principles calculations and Sec. V summarizes the results.

II. EXPERIMENT

In contrast to most studies dealing with Fe(001), which use either a whisker crystal or a thin film evaporated *in situ* on a suitable substrate like MgO(001), we used a bulk Fe single crystal. Prior to the experiments carried out at the ID03 beamline[18,19] of the European Synchrotron Radiation Facility (ESRF) in Grenoble (France), the Fe(001) crystal ($\varnothing=9$ mm) was prepared during several weeks in our home laboratory, following the procedure described by Kirschner[20] to achieve a surface free of contaminants within the limits of Auger-electron spectroscopy. Surface long-range order was checked by STM. The image shown in Fig. 1 was taken in constant-current mode at $I=0.5$ nA using a bias voltage $U=-0.3$ V. The width of some terraces approaches 500 nm, a value which even exceeds those usually observed for Fe-whisker crystals.

The SXRD experiments were carried out using a six-circle ultrahigh-vacuum diffractometer operated in the z-axis mode. The intensity distribution along the integer order crystal truncation rods (CTRs) was measured under grazing incidence ($\alpha_i=1°$) of the incoming x-ray beam ($\lambda=0.69$ Å) by rotating the sample about its surface normal. The angle α_i was chosen well above the critical angle of total reflection ($\alpha_c\approx0.14°$) in order to avoid systematic errors due to possible small sample misalignment.

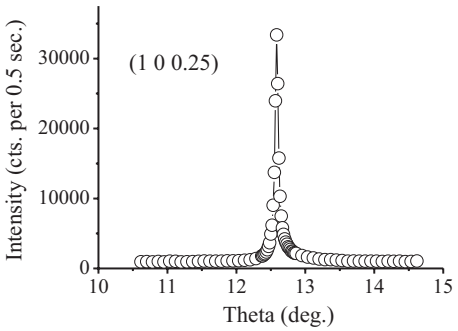

FIG. 2. Transverse scan across the (1 0 0.25) CTR reflection close to the (1 0 0) antiphase condition. The full width at half-maximum is equal to 0.05°.

The CTRs (Refs. 21 and 22) arise due to the truncation of the crystal, which makes the reflection index, $\ell=q_z/c^*$, a continuous parameter. Here, q_z and c^* represent the momentum transfer normal to the surface and the reciprocal lattice unit, respectively. Figure 2 shows for uncovered Fe(001) a transverse scan across the (1 0 0.25) reflection close to the (100) antiphase condition. Transverse scans mainly probe the width of the angular mosaic distribution. We find a full width at half-maximum of 0.05°, a value which is excellent for metal crystals.

Two kinds of samples were prepared: (i) the as-deposited sample, where oxygen was dosed at a partial pressure of $pO_2\approx5\times10^{-9}$ mbar with the sample kept at room temperature. Simultaneously the (1 0 0.25) CTR intensity was monitored until its saturation was achieved; (ii) the annealed sample, which is prepared by annealing the as-deposited one at 500 °C for 1 min.

Figure 3 shows the normalized (1 0 0.25) reflection intensity versus time. Dosing starts after about $t=100$ s (see arrow) and is continued until $t=1200$ s, where the signal is close to saturation at about 10% of the initial value. The total oxygen exposure is approximately equal to 4.2 L.

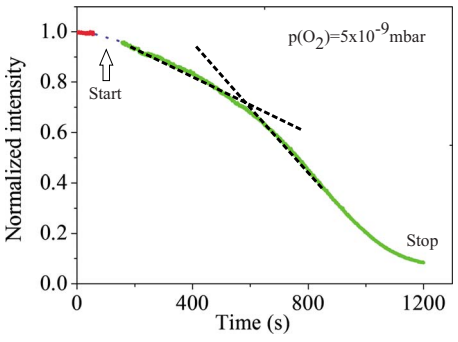

FIG. 3. (Color online) (1 0 0.25) reflection intensity versus time during oxygen exposure of Fe(001) at room temperature. The arrow indicates the beginning of the exposure at about $t=100$ s. Within the gap no SXRD data could be collected due to access to the experimental hutch. Dashed lines indicate the change in the slope taking place at about $t=600$ s (≈2 L).

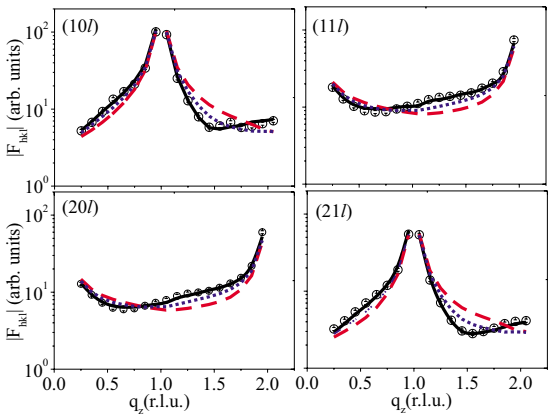

FIG. 4. (Color online) Measured (symbols) and calculated (lines) $|F|$ versus q_z along several CTRs for the annealed sample. The black line corresponds to the best fit; blue (dotted) and red (dashed) lines represent calculated $|F|$'s for 8% and 0% expansion of d_{12}.

III. DATA ANALYSIS AND STRUCTURE MODELS

Large SXRD data sets were collected for both samples, each consisting of about 300 reflections reducing to 180 symmetry independent reflections along nine CTRs after averaging using the plane group symmetry $p4mm$. The structure factor intensities ($|F|^2$) were derived by multiplying the integrated reflection intensities by geometric correction factors as described in Refs. 23–26. Standard deviations were derived from the reproducibility of symmetry equivalent reflections. Values in the 9–15 % regime were found (based on $|F|^2$).

Symbols correspond to experimental structure factors ($|F|$) for the annealed (Fig. 4) and the as-deposited (Fig. 5) samples. The overall shape of the CTRs along q_z with conditions $h+k$=even on one hand and $h+k$=odd on the other hand is identical. This is because only high-symmetry atomic sites within the unit cell (plane group $p4mm$) are occupied. Standard deviations are represented by the error bars. Solid lines represent the calculated $|F|$ values based on structure models, which will be discussed below.

The structure optimization was carried out by least-squares refinement using the program "PROMETHEUS,"[27] modified to include CTR reflections. Direct eye inspection of the best fits (solid black lines) in Figs. 4 and 5 reveals that high-quality fits could be achieved. The fit quality is quantified by the unweighted residuum (R_u) or the goodness of fit (GOF) parameter.[28] Excellent values as low as R_u=0.05 and GOF=1.3 were achieved for the annealed sample. For the as-deposited sample, the fit quality is somewhat worse (R_u =0.15 and GOF=1.7), which we attribute to the complicated disordered character of the surface.

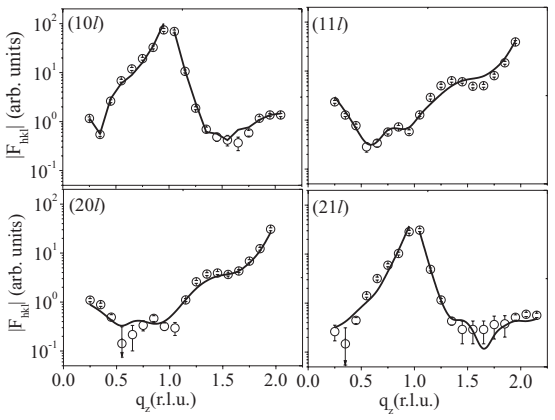

FIG. 5. Measured (symbols) and calculated (lines) $|F|$ versus q_z along several CTRs for the as-deposited sample.

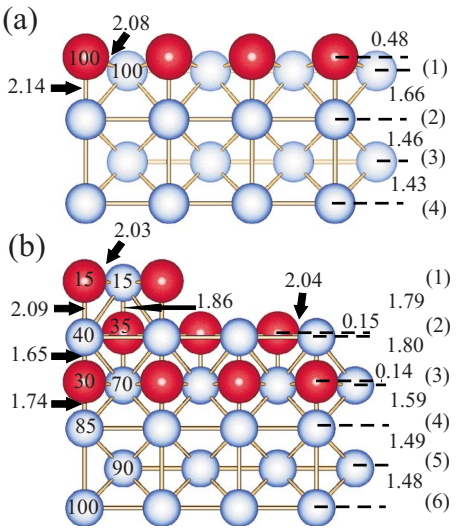

FIG. 6. (Color online) Side view of the structure model for (a) the annealed and (b) the as-deposited samples. Dark (red) and bright (blue) spheres represent oxygen and Fe atoms, respectively. Distances are given in angstrom units; numbers within spheres represent occupancy factors in percent of 1 ML. Layers are numbered on the right.

Figure 6 shows in side view the structure models for the annealed [Fig. 6(a)] and the as-deposited [Fig. 6(b)] samples. Dark (red) and bright (blue) balls represent oxygen and Fe atoms, respectively. Due to the high symmetry of the structure, only the z parameters of the atoms need to be refined. Additional variables were an overall Debye parameter representing disorder ($B=8\pi^2\langle u^2\rangle$, where $\langle u^2\rangle$ is the mean-square displacement) and the occupancy factors of the oxygen (θ_O) and Fe (θ_{Fe}) atoms. Numbers within the spheres represent θ_O and θ_{Fe} in percent of a ML. We estimate the uncertainty for θ to lie in the 10–15 percentage point range. At most five layers were involved in the structure optimization (as-deposited sample); thus, the number of refined parameters is below 15 (only seven for the annealed sample). At first, we discuss the annealed sample.

A. Annealed sample

We find a complete ML of oxygen atoms located in hollow sites at $d_{(O\text{-}Fe)}=0.48\pm0.08$ Å above the first Fe layer (no subsurface oxygen is found). Furthermore, d_{12} is expanded to 1.66 ± 0.02 Å, corresponding to a 16% increase relative to the bulk value. Within the error bars (≈0.03 Å) deeper layers are not relaxed.

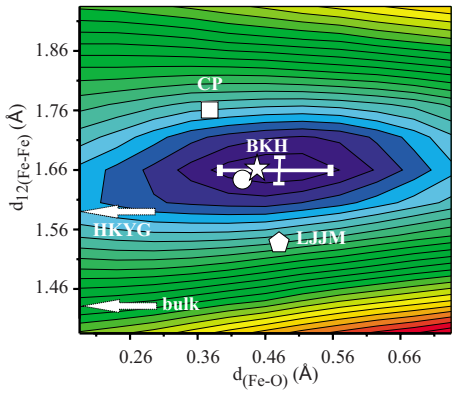

FIG. 7. (Color online) Contour plot of R_u versus d_O, and d_{12}. The minimum (blue, dark) in R_u is at 0.05; the level spacing equals ΔR_u=0.01 (maximum at lower right, red color at R_u=0.31). Previous experimental and theoretical studies are indicated CP: Ref. 11, LJMM: Ref. 9, HKYG: Ref. 12, and BKH: Ref. 3. The circle refers to the theoretical result of this study.

Figure 7 shows a contour plot of R_u versus d_{12} and $d_{(O\text{-}Fe)}$. Literature values are also reported to allow direct comparison. The minimum which is indicated by the intersection of the bars corresponds to R_u=0.05. The contour line spacing is equal to ΔR_u=0.01. The bars represent the estimated uncertainty for the determination of d_{12} and $d_{(O\text{-}Fe)}$, with the latter being about a factor of 4 larger due to the small scattering amplitude of oxygen. Our value of d_{12} is larger than the experimentally derived ones of Legg *et al.*[9] (1.54 Å; 7.5%) and Headrick *et al.*[12] (1.59 Å; 11%), but matches with that calculated by Blonski *et al.*[3]

In order to demonstrate the significance of our results we also show in Fig. 4 calculations of the structure factors where d_{12} was fixed to only +8% (blue line) and ±0% (red line) with respect to the bulk. Pronounced differences between calculated and the observed structure factor amplitudes are observed. It is well known that surface relaxations induce an asymmetry of the CTR intensity with respect to the antiphase condition.[22] In the case of an expansion the CTR minimum shifts to lower q_z, which is clearly reflected in Fig. 4. The best fit (solid line) corresponds to an expansion of 16%.

In a second step we demonstrate that the data are accurate enough to allow the determination of the oxygen occupancy (θ_O). In Fig. 8(a) R_u is plotted versus θ_O, while all other parameters are allowed to vary, i.e., correlation effects are included. There is a clear minimum at $\theta_O=1.1\pm0.2$. Certainly, an occupancy factor larger than 1.0 is physically meaningless, but within an error bar of 20% for θ_O the result indicates that the hollow sites are fully covered by oxygen. Notably, there is no large correlation between the structural parameters in general, which is a favorable condition ensuring rapid convergence of the least-squares refinement.

One exception to this rule is the Debye parameter of oxygen, which is highly correlated with the occupancy factor (θ_O) as shown in Fig. 8(b). The variation of the scattered intensity $I(hkl)$ on θ_O is compensated by a corresponding variation of B via the relation $I(hkl) \propto \exp[-B \sin^2(\Theta)/\lambda^2]$, where Θ is the Bragg angle. If θ_O is set to values below about 0.70 ML, B even adopts unphysical negative values.

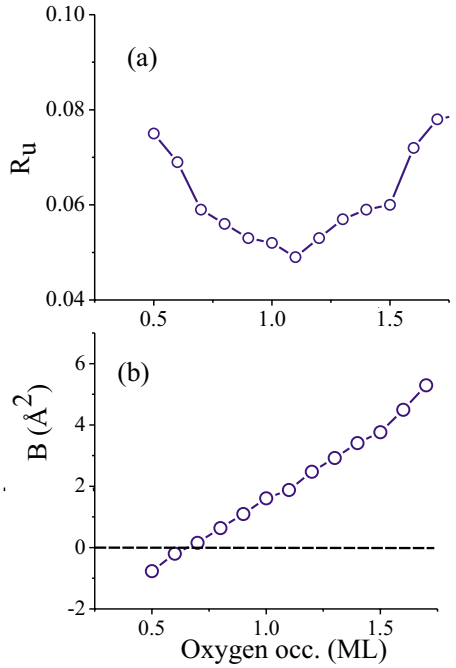

FIG. 8. (Color online) (a) Unweighted residuum (R_u) and (b) Debye parameter (B) of oxygen versus oxygen occupancy for the annealed sample.

Thus, to first approximation θ_O=0.7 can be viewed as the lower limit. At the best fit value $\theta_O \approx 1$, B(O) is equal to 1.7 Å^2 ($\sqrt{\langle u^2 \rangle}$=0.14 Å), a value typically seen for surface atoms at room temperature.

Compared with previous experimental results our d_{12} value is significantly larger, probably related to different preparation procedures. For instance, in the LEED study of Legg *et al.*[9] no annealing after oxygen exposure is reported. Direct eye inspection of the CTRs in Figs. 4 and 5 shows clear differences between the annealed and the as-deposited samples. In addition to overall lower values of $|F|$ in the regime between the bulk Bragg reflections ($h+k+\ell=2n$, n =integer), the CTRs of the as-deposited sample also exhibit an oscillatory intensity variation. This directly points to a rough surface where several layers contribute to the scattered intensity. In the following the analysis of the as-deposited sample is discussed.

B. As-deposited sample

The structure of the as-deposited sample is characterized by two layers of an FeO-like phase. As for the annealed sample we estimate the uncertainty for the determination of θ to lie in the 10–15 percentage point range; therefore, the small fraction of the third FeO layer is within the uncertainty. The oxygen occupancy in the first two layers is equal to 30–40 %. We also find roughening of the Fe surface represented by occupancy factors θ_{Fe} below 100% for the Fe layers in the interface region [layers (3)–(5)]. Notably, the "mass balance" is preserved in that the sum of the occupancies θ_{Fe} in the incomplete layers (1)–(5) is equal to 3.00 ML (integer). The total amount of oxygen is equal to 0.8 ML. Within the experimental uncertainty it is approximately 1

ML, which is the value attributed to the saturation of the surface with oxygen.

Based on the SXRD uptake curve shown in Fig. 3, no clear-cut separation between oxygen adsorption [regime (i) according to Sakisaka *et al.*[17]] and the beginning of the oxide formation [regime (ii)] can be made. There seems to be some change in the slope of the reflection intensity at $t=600$ s (corresponding to 500 s dosing time ≈ 2 L) as emphasized by the dashed lines in Fig. 3. The changing slope might tentatively be interpreted by the beginning of roughening related to the transition between regimes (i) and (ii), but an unambiguous assignment is not possible. Thus, we may speculate that no sharp transition exists between regimes (i) and (ii).

In general, we observe an expansion of the interlayer spacings with respect to bulk Fe. The distances between the pure Fe layers (d_{45} and d_{56}) are only slightly expanded to 1.48 and 1.49 Å, respectively, while d_{34} involving the lowest Fe layer occupied by oxygen is expanded to $d_{34}=1.59$ Å (+11%), very similar to the value reported by Headrick *et al.*[12] The distances between the upper layers further increase ($d_{23}=1.80$ Å), which is a consequence of the FeO structure involving Fe-O bonds with a minimum length of around 1.7 Å (error bars for the distance determination are about 0.1 Å). The FeO island formation also limits the rumpling within each FeO layer to very low values [≈ 0.15 Å in layer (2)] as compared to the adsorption height $d_{(\mathrm{O\text{-}Fe})}$ in the 0.4–0.5 Å range reported for oxygen on the bare Fe(001) surface.

The disordered nature of the as-deposited sample is also reflected in the large values of B in the range between 3 and 9 Å^2, corresponding to root-mean-square displacements $U=\sqrt{\langle u^2\rangle}$ of 0.19–0.34 Å, whereas thermal vibration amplitudes are usually in the range of 0.1 Å. The enhanced B factors are therefore attributed to static disorder, most likely due to some rumpling within layers (1)–(3) which are only partially filled by oxygen. The Fe atoms are expected to relax differently depending on whether they are in an oxygen environment or not.

In summary, the structure after dosing of about 4 L at room temperature is characterized by about two layers of an FeO-like phase which cover the Fe(001) surface to about 30–40 %. On the remaining Fe(001) surface holes are created to supply the amount of Fe necessary to form the oxide.

IV. THEORY

Our experimental results are complemented by first-principles calculations using the Vienna *ab initio* simulation package (VASP), well known for providing precise total energies and forces.[29] We used all-electron projector-augmented-wave potentials[30] and a spin-polarized generalized gradient approximation.[31] First, we calculated the equilibrium lattice constant for bulk Fe, which is found to be 2.833 Å, i.e., 1.1% smaller than that known for body-centered-cubic (bcc) Fe (2.866 Å). The calculated equilibrium lattice constant was used in the simulations of the surface structure using a slab of nine Fe layers separated by a vacuum layer of 17 Å and repeated periodically throughout space.

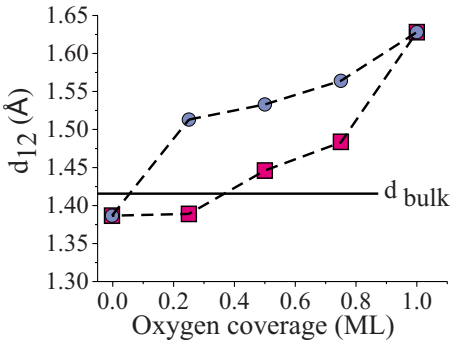

FIG. 9. (Color online) Calculated local values of d_{12} for 0.0, 0.25, 0.50, 0.75, and 1.00 ML coverage of oxygen. The large (circles) and low (squares) values are related to maximum and minimum values within the supercell. The dashed line is a guide to the eye.

We calculate $d_{(\mathrm{O\text{-}Fe})}=0.43$ Å and $d_{12}=1.63$ Å very similar to those of Blonski *et al.* ($d_{(\mathrm{O\text{-}Fe})}=0.45$ Å and $d_{12}=1.66$ Å) who used the same method and the same form of the generalized gradient approximation but ultrasoft pseudopotentials and a smaller slab of iron layers for the surface simulation.[3] In Fig. 7 Blonski's and our structure parameters are represented by the star and circle, respectively. Within the experimental error bars they agree with the SXRD results.

One main result of this study is that the oxygen induced expansion of d_{12} is larger than previously reported. One possible reason for this discrepancy might lie in a less than complete oxygen ($\theta_{\mathrm{O}}<1$ ML) coverage leading to a smaller expansion of d_{12} on average. To elucidate this effect in more detail we have carried out calculations using a (2×2) supercell successively filled by 0, 1, 2, 3, and 4 oxygen atoms corresponding to 0.00, 0.25, 0.50, 0.75, and 1.00 ML oxygen coverage [in the 0.5 ML case a $c(2\times 2)$ geometry is considered]. Results are summarized in Fig. 9 in which squares and circles represent the minimum and maximum values of d_{12} within the supercell.

For uncovered Fe(001) ($\theta_{\mathrm{O}}=0$), the top layer spacing is calculated to be contracted to $d_{12}=1.384$ Å ($\approx -2\%$ relative to the theoretical bulk lattice constant and $\approx -3.5\%$ relative to that of the bcc Fe crystal). Comparison with the LEED study by Legg *et al.*[32] for uncovered Fe(001) (-1.4 ± 3 %) indicates reasonable agreement within the (relatively large) experimental uncertainty. The calculations tend to yield distances too short in general, which can be explained by limitations of the density-functional theory.

For the partially filled oxygen layer we find different values for d_{12} depending on whether a hollow site is occupied by oxygen or not. In general if a site is occupied, the corresponding local value of d_{12} is enhanced relative to d_{12} at an unoccupied site. The difference between the minimum and the maximum values of d_{12} within the (2×2) supercell is largest at 0.25 ML coverage (0.12 Å). It decreases to 0.09 and 0.08 Å for 0.5 and 0.75 ML, while for the fully covered surface a homogeneous expansion to 1.63 Å is derived (see Fig. 9). Although this value is lower than 1.66 Å as derived by the SXRD analysis, it is almost in perfect agreement on a relative scale, i.e., when referenced to the calculated bulk

spacing of 1.414 Å. In summary, the calculations indicate that a less than complete oxygen coverage leads to a shorter (average) spacing. Agreement with the previous LEED study[9,10] is achieved at a coverage of 75%.

Apart from d_{12} we have also investigated the adsorption height of oxygen above the first Fe layer. At a coverage above 0.50 ML the average $d_{(\mathrm{O\text{-}Fe})}$ remains stable at 0.43 Å, which is explained by strong chemical bond between O and Fe surface atoms.

V. SUMMARY AND CONCLUSIONS

In summary we have presented a SXRD analysis of the old standing problem of the atomic geometry of the O/Fe(001)-p(1×1) surface. Deposition of several langmuirs of oxygen at room temperature induces the formation of FeO-like islands two ML thick occupying about 30–40 % of the surface area corresponding to an oxygen coverage close to 1 ML. Sample annealing induces surface flattening and the formation of a well-ordered structure in which a complete ML of oxygen atoms resides in hollow sites. Our SXRD data are accurate enough to allow a precise determination of the oxygen occupancy within an uncertainty of 20% of a ML. We find that oxygen atoms are located 0.48 Å above the surface plane and that the top Fe-interlayer spacing is expanded to 1.66 Å corresponding to a 16% expansion relative to the bulk value in good agreement with DFT calculations.

Our findings are especially important in the context of recent experimental and theoretical studies of the magnetic properties of the oxygen covered Fe(001) surface[3,7] showing a delicate dependence of the oxygen induced spin-polarized states near the Fermi level, the enhancement of the surface magnetic moments, and the exchange splitting. A more detailed analysis of the correlation between the structure parameters and the surface magnetic properties will be published elsewhere.[33]

ACKNOWLEDGMENTS

We (H.L.M., S.S.P., K.M., and N.J.) are grateful to the ESRF staff for their help and hospitality during our stay in Grenoble. This work is supported by the Sonderforschungsbereich SFB 762, "Functionality of Oxidic Interfaces." The calculations were performed at the John von Neumann Institute in Jülich.

*hmeyerhm@mpi-halle.mpg.de

[1] H. Huang and J. Hermanson, Phys. Rev. B **32**, 6312 (1985).
[2] M. Getzlaff, J. Bansmann, and G. Schönhense, Fresenius' J. Anal. Chem. **353**, 743 (1995).
[3] P. Blonski, A. Kiejna, and J. Hafner, Surf. Sci. **590**, 88 (2005).
[4] F. Bisio, R. Moroni, M. Canepa, L. Mattera, R. Bertacco, and F. Ciccacci, Phys. Rev. Lett. **83**, 4868 (1999).
[5] R. Bertacco and F. Ciccacci, Phys. Rev. B **59**, 4207 (1999).
[6] M. Nyvlt, F. Bisio, J. Franta, C. L. Gao, H. Petek, and J. Kirschner, Phys. Rev. Lett. **95**, 127201 (2005).
[7] A. Tange, C. L. Gao, B. Y. Yavorsky, I. V. Maznichenko, C. Etz, A. Ernst, W. Hergert, I. Mertig, W. Wulfhekel, and J. Kirschner (unpublished).
[8] A. Winkelmann, D. Hartung, H. Engelhard, C.-T. Chiang, and J. Kirschner, Rev. Sci. Instrum. **79**, 083303 (2008).
[9] K. O. Legg, F. Jona, D. W. Jepsen, and P. M. Marcus, Phys. Rev. B **16**, 5271 (1977).
[10] F. Jona and P. M. Marcus, Solid State Commun. **64**, 667 (1987).
[11] S. R. Chubb and W. E. Pickett, Phys. Rev. Lett. **58**, 1248 (1987).
[12] R. L. Headrick, P. Konarski, S. M. Yalisove, and W. R. Graham, Phys. Rev. B **39**, 5713 (1989).
[13] C. F. Brucker and T. N. Rhodin, Surf. Sci. **57**, 523 (1976).
[14] J.-P. Lu, M. R. Albert, S. L. Bernasek, and D. Dwyer, Surf. Sci. **215**, 348 (1989).
[15] F. Bonell, A. M. Bataille, S. Andrieu, C. Tiusan, B. Kierren, G. Lengaigne, and D. Lacour, Eur. Phys. J.: Appl. Phys. **43**, 357 (2008).
[16] F. Bonell, S. Andrieu, A. M. Bataille, C. Tiusan, and G. Lengaigne, Phys. Rev. B **79**, 224405 (2009).
[17] Y. Sakisaka, T. Miyano, and M. Onchi, Phys. Rev. B **30**, 6849 (1984).
[18] S. Ferrer and F. Comin, Rev. Sci. Instrum. **66**, 1674 (1995).
[19] O. Balmes, R. van Rijn, D. Wermeille, A. Resta, L. Petit, H. Isern, T. Dufrane, and R. Felici, Catal. Today **145**, 220 (2009).
[20] J. Kirschner, Surf. Sci. **138**, 191 (1984).
[21] I. K. Robinson, Phys. Rev. B **33**, 3830 (1986).
[22] I. K. Robinson and D. J. Tweet, Rep. Prog. Phys. **55**, 599 (1992).
[23] R. Feindenhans'l, Surf. Sci. Rep. **10**, 105 (1989).
[24] C. Schamper, H. L. Meyerheim, and W. Moritz, J. Appl. Crystallogr. **26**, 687 (1993).
[25] E. Vlieg, J. Appl. Crystallogr. **30**, 532 (1997).
[26] N. Jedrecy, J. Appl. Crystallogr. **33**, 1365 (2000).
[27] U. H. Zucker, E. Perenthaler, W. F. Kuhs, R. Bachmann, and H. Schulz, J. Appl. Crystallogr. **16**, 358 (1983).
[28] R_u is defined as $R_u=\Sigma\big||F^{\mathrm{obs}}|-|F^{\mathrm{calc}}|\big|/\Sigma|F^{\mathrm{obs}}|$ with F^{obs} and F^{calc} as the observed and calculated structure factors, respectively. For GOF see Ref. 23.
[29] G. Kresse and J. Hafner, J. Phys.: Condens. Matter **6**, 8245 (1994).
[30] P. E. Blöchl, Phys. Rev. B **50**, 17953 (1994).
[31] J. P. Perdew, K. Burke, and M. Ernzerhof, Phys. Rev. Lett. **77**, 3865 (1996).
[32] K. O. Legg, F. Jona, D. W. Jepsen, and P. M. Marcus, J. Phys. C **10**, 937 (1977).
[33] C. Etz, A. Ernst, H. L. Meyerheim, and W. Wulfhekel (unpublished).